Journal of the Serbian Chemical Society
JSCS-info@shd.org.rs • www.shd.org.rs/JSCS
J. Serb. Chem. Soc. *81* (11) 1263–1272 (2016) UDC 519.677:535.33–31+546.472'742'982:
JSCS–4925 547.496.3:538.913
Original scientific paper

DFT/TD-DFT study on the spectroscopic properties of zinc(II), nickel(II), and palladium(II) metal complexes with a thiourea derivative

XIN WANG[1], JIEQIONG LI[1], LI WANG[1]*, WENPENG WU[1]**, ZHENG DU[2] and WENLONG LUO[2]

[1]*Institute of Environmental and Analytical Sciences, College of Chemistry and Chemical Engineering, Henan University, Kaifeng 475004, Henan, China and* [2]*National Supercomputing Center in Shenzhen, Shenzhen, Guangdong, 518055, China*

(Received 6 May, revised 6 July, accepted 26 July 2016)

Abstract: The geometries, electronic structures, and spectral properties of three metal complexes $Zn(C_{10}H_{12}N_3OS)_2$ (**1**), $Ni(C_{10}H_{12}N_3OS)_2$ (**2**) and $Pd(C_{10}H_{12}N_3OS)_2$ (**3**) with *N*-2-pyridinylmorpholine-4-carbothioamide as a ligand were investigated by means of the DFT (density functional theory) and TD-DFT (time-dependent density functional theory) methods. Complex **1** has a distorted tetrahedral geometry, while complexes **2** and **3** present a distorted square-planar coordination environment. In the simulated range, the spectrum of complex **1** has five obvious absorption peaks and one of them has the strongest intensity. The latter two complexes have one more absorption peak and a shoulder with similar intensity. Moreover, the strongest peak of complexes **2** and **3** is blue-shifted as compared with that of complex **1**.

Keywords: TD-DFT theory; electronic spectra; electronic structures; thiourea.

INTRODUCTION

Thiourea and its derivatives have received considerable attention during the past two decades because of their versatile biological activity and potential applications in industry and agriculture.[1,2] In addition, they are efficient complexing agents for metal ions and are widely employed as ligands in coordination chemistry.[3] The presence of hard N- and O- and/or soft S-donor atoms in the backbones allows them to react easily with both transition group and main group metal ions, leading to stable metal complexes. Some of them have been testified as exhibiting significant physical, chemical, and biological properties. Complexes of thiourea with Zn(II) ion have been proved to be the potential starting materials for the fabrication of thin metal sulfide films possessing semicon-

* Corresponding authors. E-mail: (*)chemwangl@henu.edu.cn; (**)wenpengwu@126.com
doi: 10.2298/JSC160506071W

ducting properties.[4] The nickel(II) complexes containing *N*-substituted derivatives of thiourea were found to exhibit excellent DNA/protein binding and antioxidant properties.[5] In addition, a number of Pt(II) complexes have been used as clinical antitumor drugs. Recently, much more attention has been turned to explore new metal complexes of thiourea derivatives with greater potency and less toxicity than current clinical drugs. Therefore, Pd(II) complexes became the new focus of attention owing to their wide spectrum of medicinal properties.

In 2012, Orysyk *et al.*[6] synthesized and characterized three new Zn(II), Ni(II), and Pd(II) complexes with *N*-2-pyridinylmorpholine-4-carbothioamide as the ligand. Based on the experimental information, the ground electronic states of three metal complexes, **1**–**3**, were theoretically investigated by the DFT method in the present work. Subsequently, the vertical excitation energies were evaluated by the TD-DFT method. The general aim was to understand deeply the properties of the absorption spectra and to elucidate the influence of the structures on the absorption spectra.

COMPUTATIONAL DETAILS

The geometries of three complexes were optimized by three DFT levels of theory without any symmetry restriction, *i.e.*, M06,[7] B3LYP (Becke's three-parameter non-local--exchange functional with the nonlocal correlation of Lee–Yang–Parr),[8,9] and B3PW91 (Beck's three-parameter nonlocal-exchange functional with the generalized gradient approximation (GGA) Perdew–Wang 91 correlation functional)[10] methods. The 6-31+G(d) basis set was employed for non-metal atoms. The "double-ζ" quality basis set LANL2DZ associated with quasi-relativistic pseudo-potentials proposed by Hay and Wadt[11,12] served for the metal atoms, in which the LANL2DZ basis set was adopted for the valence electrons and the pseudo potentials were used for the core electrons.

Based on the M06 optimized geometries, the absorption spectra of the three metal complexes were calculated at the TD–M06 level of theory with the identical basis set. The polarized continuum model (PCM)[13] with dimethylformamide was employed to assess the solvent effect on the spectral properties.

To verify the reliability of the TDDFT/M06 method, the absorption spectrum of complex **2** was also evaluated by the statistical averaging of the (model) orbital potentials (SAOP)[14,15] in combination with the double-ζ plus polarization (DZP) basis set implemented in the program package ADF.[16,17] As shown in Fig. S-1 of the Supplementary material to this paper, the absorption features simulated at the TD-DFT/SAOP level present inconsistencies with the experimental values.[6] There was no absorption peak in the range of 230–240 nm. In contrast, one moderate absorption bank (239 nm) was reported in the experiment. Therefore, the TDDFT/M06 functional was more reliable for this system and became the final choice to calculate the vertical excitation energies.

RESULTS AND DISCUSSION

Geometry structures

The optimized structures of the investigated metal complexes are shown in Fig. 1. Furthermore, the schematic structures together with labeling the Py (pyridyl)

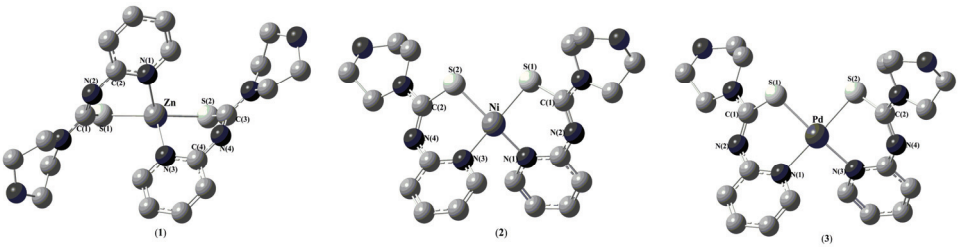

Fig. 1. The optimized ground-state structures for complexes $Zn(C_{10}H_{12}N_3OS)_2$ (**1**), $Ni(C_{10}H_{12}N_3OS)_2$ (**2**) and $Pd(C_{10}H_{12}N_3OS)_2$ (**3**). The hydrogen atoms are omitted for clarity.

and Mor (morpholine) rings and key atoms are presented in Fig. S-2 of the Supplementary material. Before starting the following discussions, three issues deserve to be considered. First, since the accurate geometries are essential to study the spectral properties, selecting a more suitable method to optimize the structure is the principal problem. The DFT method has revolutionized the role of theory by providing accurate first-principle predictions of critical properties since its computational costs are low compared to *ab initio* methods. However, a functional that is suitable for all systems is unknown and is unlikely to be discovered in the near future. Three DFT functionals, *i.e.*, M06, B3LYP, and B3PW91 were chosen in this work. The geometric parameters of the three studied metal complexes are listed in Tables I–III, respectively, and associated with the experimental values.[6] It shows that the results computed with the different functionals are similar to each other. Furthermore, the mean unsigned error (*MUE*) between the theoretical values and the experimental ones were calculated (see Table S-I of the Supplementary material). It is found that the M06 functional was relatively a little better than the other two functionals. Hence, M06 method, which is reported to be one of the most successful functionals for the metal complexes and has been extensively used in organometallic systems,[18–21] was confirmed to perform the following studies. The corresponding Cartesian coordinations of the ground state structures for complexes $Zn(C_{10}H_{12}N_3OS)_2$ (**1**), $Ni(C_{10}H_{12}N_3OS)_2$ (**2**) and $Pd(C_{10}H_{12}N_3OS)_2$ (**3**) are listed in Table S-II of Supplementary material.

TABLE I. Calculated bond lengths (Å) and angles (°) for complex $Zn(C_{10}H_{12}N_3OS)_2$ (**1**) by the B3LYP, B3PW91 and M06 methods with the 6-31+G(d)-LANL2DZ basis set together with the experimental values.[6] The absolute errors are listed in parentheses

Bond	B3LYP	B3PW91	M06	Exp.
Zn–N(1)	2.1189(0.0937)	2.1041(0.0789)	2.1073(0.0821)	2.0252
Zn–N(3)	2.1187(0.0865)	2.1041(0.0719)	2.1073(0.0751)	2.0322
Zn–S(1)	2.3705(0.0944)	2.3553(0.0792)	2.3427(0.0666)	2.2761
Zn–S(2)	2.3704(0.0805)	2.3552(0.0653)	2.3428(0.0529)	2.2899
S(1)–C(1)	1.7764(0.0091)	1.7654(–0.0019)	1.7781(0.0108)	1.7673
S(2)–C(3)	1.7764(0.0101)	1.7654(–0.0009)	1.7781(0.0118)	1.7663
N(2)–C(1)	1.3145(0.0091)	1.3127(0.0073)	1.3067(0.0013)	1.3054

TABLE I. Continued

Bond	B3LYP	B3PW91	M06	Exp.
N(4)–C(3)	1.3145(0.0121)	1.3127(0.0103)	1.3067(0.0043)	1.3024
N(1)–Zn–S(1)	95.55(–1.63)	95.67(–1.51)	95.13(–2.05)	97.18
N(3)–Zn–S(1)	116.65(6.26)	116.56(6.17)	115.15(4.76)	110.39
N(1)–Zn–S(2)	116.64(8.02)	116.56(7.94)	115.14(6.52)	108.62
N(3)–Zn–S(2)	95.57(0.22)	95.67(0.32)	95.13(–0.22)	95.35
S(1)–Zn–S(2)	122.99(–0.97)	122.47(–1.49)	131.75(7.79)	123.96
C(1)–N(2)–C(2)–N(1)	–29.99(11.11)	–30.62(10.48)	–38.52(2.58)	–41.10
C(3)–N(4)–C(4)–N(3)	–29.95(16.15)	–30.63(15.47)	–38.50(7.60)	–46.10

TABLE II. Calculated bond lengths (Å) and angles (°) for complex $Ni(C_{10}H_{12}N_3OS)_2$ (**2**) by the B3LYP, B3PW91 and M06 methods with the 6-31+G(d)-LANL2DZ basis set together with the experimental values.[6] The absolute errors are listed in parentheses

Bond	B3LYP	B3PW91	M06	Exp.
Ni–N(1)	1.9569(0.0346)	1.9357(0.0134)	1.9322(0.0099)	1.9223
Ni–N(3)	1.9568(0.0225)	1.9357(0.0014)	1.9322(–0.0021)	1.9343
Ni–S(2)	2.2342(0.0880)	2.2129(0.0667)	2.2041(0.0579)	2.1462
Ni–S(1)	2.2342(0.0503)	2.2129(0.0290)	2.2041(0.0202)	2.1839
S(1)–C(1)	1.7688(0.0024)	1.7584(–0.0080)	1.7630(–0.0034)	1.7664
S(2)–C(2)	1.7688(0.0255)	1.7584(0.0151)	1.7630(0.0197)	1.7433
N(2)–C(1)	1.3186(0.0152)	1.3169(0.0135)	1.3133(0.0099)	1.3034
N(4)–C(2)	1.3186(0.0012)	1.3169(–0.0005)	1.3133(–0.0041)	1.3174
N(1)–Ni–N(3)	93.29(–1.16)	93.17(–1.28)	92.47(–1.98)	94.45
N(1)–Ni–S(2)	168.62(–0.30)	168.91(–0.01)	168.74(–0.18)	168.92
N(1)–Ni–S(1)	90.61(0.59)	90.75(0.73)	90.99(0.97)	90.02
N(3)–Ni–S(2)	90.63(–3.05)	90.75(–2.93)	90.99(–2.69)	93.68
N(3)–Ni–S(1)	168.65(–0.58)	168.91(–0.32)	168.74(–0.49)	169.23
S(2)–Ni–S(1)	87.58(4.26)	87.31(3.99)	87.65(4.33)	83.32

Next, are the coordinated ligands present in the *cis*- or *trans*-configuration in the complexes? The complex $[Zn(C_{10}H_{12}N_3OS)_2]$ (**1**) was located in the trans--conformation, while the other complexes $[Ni(C_{10}H_{12}N_3OS)_2]$ (**2**) and $[Pd(C_{10}H_{12}N_3OS)_2]$ (**3**) were located in the *cis*-configuration, which is consistent with the experimental observations.[6] For every complex, the other configuration failed to be located.

According to the present calculations, complex **1** presents a distorted tetrahedral coordination geometry, which is consistent with experimental and previous theoretical results.[22] Complexes **2** and **3** exhibit a square-planar coordination environment with the same bond distances of Ni(Pd)–S(1)/N(1) and Ni(Pd)–S(2)/N(3). The difference is that the angles of S(2)–Pd–N(1) and S(1)–Pd–N(3) for complex **3** are much closer to linear than those of complex **2**. Consequently, complex **3** shows a more nearly regular square-planar coordination conformation. The different structures of these three complexes, especially

for complex **1**, will result in discrepancies for the electronic structures and spectral properties.

TABLE III. Calculated bond lengths (Å) and angles (°) for complex $Pd(C_{10}H_{12}N_3OS)_2$ (**3**) by the B3LYP, B3PW91 and M06 methods with the 6-31+G(d)-LANL2DZ basis set together with the experimental values.[6] The absolute errors are listed in parentheses.

Bond	B3LYP	B3PW91	M06	Exp.
Pd–N(1)	2.1196(0.0534)	2.0943(0.0281)	2.1163(0.0501)	2.0662
Pd–N(3)	2.1196(0.0416)	2.0943(0.0163)	2.1163(0.0383)	2.0780
Pd–S(2)	2.3390(0.0920)	2.3162(0.0692)	2.3314(0.0844)	2.2470
Pd–S(1)	2.3391(0.0575)	2.3162(0.0346)	2.3314(0.0498)	2.2816
S(1)–C(1)	1.7737(0.0085)	1.7623(–0.0029)	1.7688(0.0036)	1.7652
S(2)–C(2)	1.7737(0.0305)	1.7623(0.0191)	1.7688(0.0256)	1.7432
N(2)–C(1)	1.3156(0.0083)	1.3143(0.0070)	1.3098(0.0025)	1.3073
N(4)–C(2)	1.3156(0.0063)	1.3143(0.0050)	1.3098(0.0005)	1.3093
N(1)–Pd–N(3)	94.61(–0.93)	94.35(–1.19)	94.58(–0.96)	95.54
N(1)–Pd–S(2)	173.52(1.31)	173.68(1.47)	172.87(0.66)	172.21
N(1)–Pd–S(1)	88.34(–3.24)	88.57(–3.01)	88.58(–3.00)	91.58
N(3)–Pd–S(2)	88.32(0.57)	88.57(0.82)	88.58(0.83)	87.75
N(3)–Pd–S(1)	173.52(1.14)	173.68(1.30)	172.87(0.49)	172.38
S(2)–Pd–S(1)	89.33(3.73)	89.08(3.48)	89.00(3.40)	85.60

Molecular orbitals

Elucidating the composition of frontier molecular orbitals (FMOs) (HOMO (H) – the highest occupied molecular orbital and LUMO (L) – the lowest unoccupied molecular orbital) is essential to cast light on the absorption spectra intrinsically. The selected FMOs compositions (including the four highest HOMOs and the three lowest LUMOs) of corresponding three metal complexes are tabulated in Tables S-III–S-V of the Supplementary material. Furthermore, selected molecular orbitals involved in the key absorptions of the studied complexes, the calculated energy levels, and the energy gaps are plotted in Fig. 2.

Now, let attention be paid to the orbital composition of the three metal complexes. The detailed orbital distribution will not be discussed individually. The common and different points among them will be emphasized. The similar points are: 1) the contribution of C atoms (C(1), C(2) and C(3)) can be neglected for all selected FMOs; 2) the electron density distributions of L+1 and L+2 are mainly distributed over the π* orbital of the Py groups (Py(A) and Py(B)); 3) the Mor groups (Mor(A) and Mor(B)) and N atoms (N(2) and N(4)) contribute little to the LUMOs. Except for the similar points, there are also different items deserving attention. One is that the Zn atom has no contribution to all selected FMOs of complex **1**, while the d orbital of the Ni or Pd atom plays an important role in complexes **2** and **3**, respectively, especially for the LUMO. The other one is that the electrons extend over the S atoms (S(1) and S(2)) in the FMOs of complexes

2 and **3** more than in complex **1**. In general, the properties of complexes **2** and **3** are more similar to each other as compared with complex **1**, which is related to their structures.

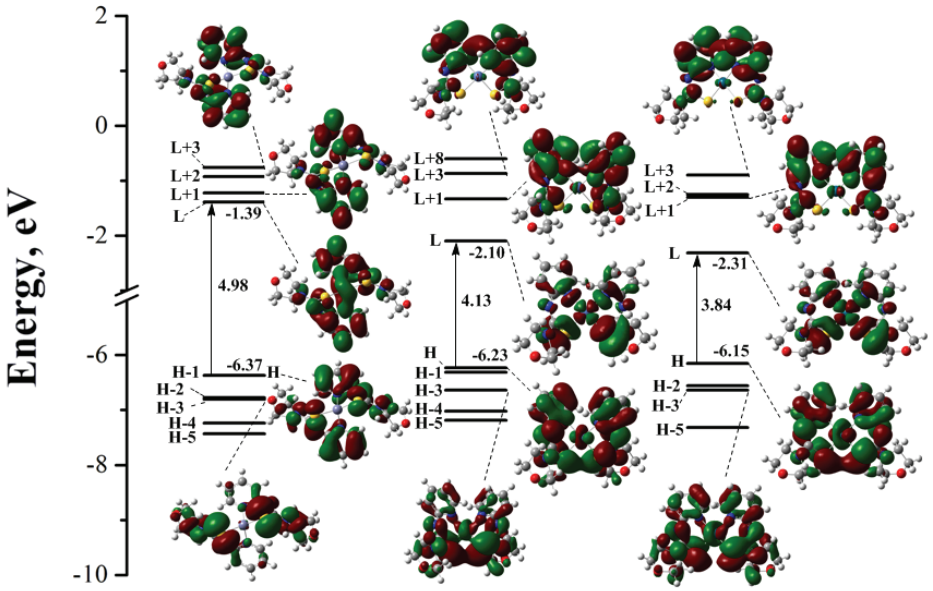

Fig. 2. Presentation of the energy levels, energy gaps, and frontier molecular orbitals involved in the absorption spectra for complexes $Zn(C_{10}H_{12}N_3OS)_2$ (**1**), $Ni(C_{10}H_{12}N_3OS)_2$ (**2**) and $Pd(C_{10}H_{12}N_3OS)_2$ (**3**).

Electronic spectra

Based on the optimized ground-state structures, the singlet→singlet absorptions of the three metal complexes in dimethylformamide (DMF) medium were simulated by the TD–M06/6-31+G(d)-LANL2DZ approach associated with the polarized continuum model (PCM). The most leading absorptions (with larger configuration interaction (*CI*) coefficients) are listed in Table IV along with items of assignment, excitation energies, oscillator strengths (*f*), and experimental values.[6] The corresponding simulated Gaussian type absorption curves are plotted in Fig. 3.

The calculated absorption spectra show one intense absorption peak for complex **1**, while there are two relatively strong peaks for complexes **2** and **3** in the range of 250–295 nm. By comparison, the calculated absorption spectra are in fairly good agreement with the experimental results.[6] For complex **1**, the experimentally determined strong absorption peak at 337 nm occurs in the same region as the calculated band at 309 nm, which mainly arises from the transition from the HOMO to LUMO. The HOMO exhibits p character of the N(2) and N(4)

TABLE IV. Calculated absorptions of the complexes $Zn(C_{10}H_{12}N_3OS)_2$ (**1**), $Ni(C_{10}H_{12}N_3OS)_2$ (**2**) and $Pd(C_{10}H_{12}N_3OS)_2$ (**3**) in dimethylformamide medium at the TD–M06 level together with the experimental values[6]

Complex	State	λ nm	f	Main onfiguration	Assignments	$\lambda_{Expt.}$ nm	$\nu_{Expt.}$ cm^{-1}
$Zn(C_{10}H_{12}N_3OS)_2$	S_2	309	0.4625	H→L (73 %)	n→π* LL/ILCT	337	29700
	S_7	275	0.2410	H→L+2 (61 %)	n→π* LL/ILCT	285	35060
	S_{19}	249	0.2080	H-4→L (43 %)	n→π* LL/ILCT	262	38200
	S_{28}	237	0.1087	H-3→L+3 (53 %)	n→π* LL/ILCT	–	–
	S_{40}	226	0.0846	H-4→L+2 (38 %)	n→π* LL/ILCT	–	–
$Ni(C_{10}H_{12}N_3OS)_2$	S_8	335	0.0595	H-3→L (34 %)	n+d→π* LL/IL/LMCT	345	28974
	S_9	323	0.0971	H→L+1 (72 %)	n+d→π* LL/IL/MLCT	320	31284
	S_{13}	293	0.2346	H-11→L (27 %)	n+d→n+d LL/IL/MLCT	290	34438
	S_{18}	281	0.1087	H-1→L+3 (49 %)	n→π* LL/ILCT	–	–
	S_{22}	268	0.1040	H-4→L+1 (36 %)	n+d→π* LL/IL/MLCT	267	37425
	S_{38}	251	0.3186	H-10→L (28 %)	n+π→n+d* LL/IL/LMCT	–	–
	S_{50}	239	0.0917	H-14→L (40 %)	n+π→n+d LL/IL/LMCT	239	41790
$Pd(C_{10}H_{12}N_3OS)_2$	S_8	327	0.0916	H→L+1 (73 %)	n+d→π* LL/IL/MLCT	333	30000
	S_{10}	303	0.1182	H-12→L (42 %)	π+d→n+d LL/IL/LMCT	–	–
	S_{14}	287	0.2293	H-2→L+1 (59 %)	n+d→π* LL/IL/MLCT	285	35060
	S_{36}	254	0.3158	H-3→L+3 (61 %)	n→π* LL/ILCT	260	38536
	S_{46}	240	0.0362	H-5→L+2 (28 %)	n+d→π* LL/IL/MLCT	238	42100

atoms and the LUMO is primarily localized on the π* of the Py(A) and Py(B) groups, so this transition is designated as n→π*. With respect to complex **2**, the absorption peaks at 251 (268) and 293 (280) nm have similar intensity to form shoulder peaks.

The two absorptions at 251 and 293 nm are mainly associated with H-10→L and H-11→L transitions, respectively, which are designated as n+π→n+d and n+d→n+d with the LL/IL/LMCT and LL/IL/MLCT characters, respectively. Com-

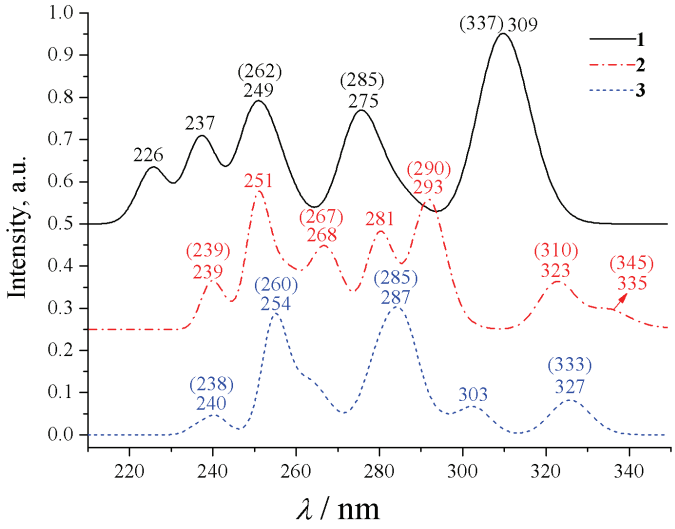

Fig. 3. Simulated absorption spectra in dimethylformamide DMF for complexes $Zn(C_{10}H_{12}N_3OS)_2$ (**1**), $Ni(C_{10}H_{12}N_3OS)_2$ (**2**), and $Pd(C_{10}H_{12}N_3OS)_2$ (**3**) from TD–M06(PCM) calculations together with the experimental values[6] in parentheses. For clarity, the oscillator strength is increased by 0.5 for $[Zn(C_{10}H_{12}N_3OS)_2]$ (**1**) and 0.25 for $[Ni(C_{10}H_{12}N_3OS)_2]$ (**2**).

plex **3** also has two shoulder peaks centered at 254 and 287 nm associated with H-3→L+3 and H-2→L+1 transitions, respectively, which are attributed to the n→π* and n+d→π* with characters of IL/LLCT and IL/LL/MLCT, respectively. The detailed transition features for the other absorption bands will not be discussed individually here. One of the distinguishable advantages of a theoretical study is their ability to separate peaks that are hard to be realized by experimental measurement. For example, complex **2** presents seven absorption peaks in the theoretically simulated wavelength range. However, two moderate absorption bands located at 281 and 251 nm were not observed experimently.[6]

Additionally, the absorption spectra for complex **2** in gas phase and in solvents (tetrahydrofuran (THF, ε = 7.426 cm^2 mol^{-1}), dichloroethane (DCE, ε = = 10.125 cm^2 mol^{-1}), and dimethylformamide (DMF, ε = 37.219 cm^2 mol^{-1})) with different polarities were investigated at the same level to explore the effect of the solvent on the absorption features. It is clear from Fig. 4 that absorption bands do not show significant solvent sensitivity to the variation of polarity. Although the intensities of the absorption peaks are strengthened with increasing solvent polarity, the positions in different solvents remain almost constant. However, the absorption curve simulated in gas phase presents distinct differences. The number of the absorption peaks is reduced and their oscillator strengths are obviously decreased. Besides, their wavelengths show a slight red shift as compared with the absorption spectra in the different solvents.

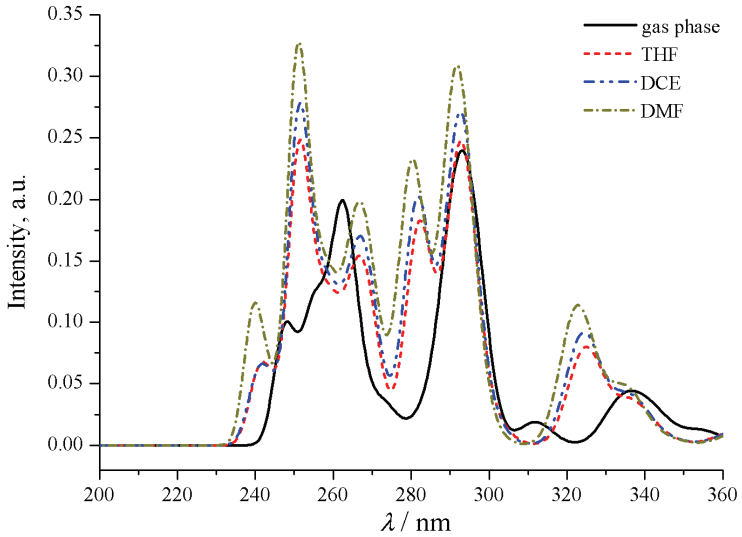

Fig. 4. Simulated absorption spectra for complex $Ni(C_{10}H_{12}N_3OS)_2$ (**2**) in the gas phase and in different solvents (THF, DCE and DMF).

CONCLUSIONS

The density functional theory and time-dependent density functional theory were used to investigate the ground-state geometries, electronic structures, and absorption spectra of three thiourea metal complexes **1**–**3**. Both the geometrical and electronic structures and the absorption properties of complexes **2** and **3** are more similar to each other relative to complex **1**. When the metal center changes from Zn to Ni/Pd, the absorption spectrum presents different features. The number of the absorption peaks increases and the strongest one is blue-shifted. Furthermore, solvents with different polarities had only a slight influence on the position and intensity of the absorption peaks. However, the absorption spectrum in gas phase showed distinct diversity.

SUPPLEMENTARY MATERIAL

The simulated absorption spectrum for complex **2** at TD-DFT/SAOP level, mean unsigned error (*MUE*) for the three different functionals and schematic structures, Cartesian coordinates of the ground state structures, molecular orbital compositions in the ground state for complexes **1**–**3** are available electronically at the pages of journal website: http://www.shd.org.rs/JSCS/, / or from the corresponding author on request.

Acknowledgements. We thank the National Supercomputing Center in Shenzhen (Shenzhen Cloud Computing Center) for providing computational resources and software. This work was financially supported by the National Natural Science Foundation of China (21376063, 21476061), the Program for the Henan Innovative Research Team in the University (15IRTSTHN005), and the Scientific Research Foundation of Henan University (B2013141, 2015YBZR009).

ИЗВОД

DFT/TDDFT СТУДИЈА СПЕКТРОСКОПСКИХ СВОЈСТАВА КОМПЛЕКСА МЕТАЛА ЦИНКА(II), НИКЛА(II) И ПАЛАДИЈУМА(II) СА ДЕРИВАТИМА ТИОУРЕЕ

XIN WANG[1], JIEQIONG LI[1], LI WANG[1], WENPENG WU[1], ZHENG DU[2] и WENLONG LUO[2]

[1]*Institute of Environmental and Analytical Sciences, College of Chemistry and Chemical Engineering, Henan University, Kaifeng 475004, Henan, China u* [b]*National Supercomputing Center, Shenzhen, Guangdong, 518055, China*

Истраживане су геометрије, електронске стрултуре и спектрална својства три метална комплекса, $Zn(C_{10}H_{12}N_3OS)_2$ (**1**), $Ni(C_{10}H_{12}N_3OS)_2$ (**2**) и $Pd(C_{10}H_{12}N_3OS)_2$ (**3**), са *N*-2-пиридинилморфолин-4-карботиоамидом као лигандом помоћу DFT (теорија функционала густине) и TD-DFT (временски зависна теорија функционала густине) метода. Комплекс **1** има изобличену геометрију тетраедра, док комплекси **2** и **3** показују изобличено квадратно-планарно координационо окружење. У симулираној области, спектар комплекса **1** има пет апсорпционих пикова и један од њих је најјачег интензитета. Друга два комплекса имају један апсорпциони пик више и раме на пику сличног интензитета. Поред тога, најјачи пикови комплекса **2** и **3** су плаво померени у поређењу са оним у комплексу **1**.

(Примљено 6. маја, ревидирано 6. јула, прихваћено 26. јула 2016)

REFERENCES

1. H. Arslan, N. Duran, N. O. Sahin, N. Kulcu, *Asian J. Chem.* **18** (2006) 1710
2. T. K. Venkatachalam, C. Mao, F. M. Uckun, *Bioorg. Med. Chem.* **12** (2004) 4275
3. S. Saeed, N. Rashid, M. Ali, R. Hussain, *Eur. J. Chem.* **1** (2010) 200
4. J. Madarász, P. Bombicz, M. Okuya, S. Kaneko, *Solid State Ionics* **141** (2001) 439
5. N. Selvakumarana, N. S. P. Bhuvaneshb, A. Endoc, R. Karvembu, *Polyhedron* **75** (2014) 95
6. S. I. Orysyk, V. V. Bon, V. I. Pekhnyo, Y. L. Zborovskii, V. V. Orysyk, M. V. Vovk, *Polyhedron* **38** (2012) 15
7. Y. Zhao, D. G. Truhlar, *Theor. Chem. Acc.* **120** (2008) 215
8. A. D. Becke, *J. Chem. Phys.* **98** (1993) 5648
9. C. Lee, W. Yang, R. G. Parr, *Phys. Rev., B* **37** (1988) 785
10. J. P. Perdew, J. A. Chevary, S. H. Vosko, K. A. Jackson, M. R. Pederson, D. J. Singh, C. Fiolhais, *Phys. Rev., B* **46** (1992) 6671
11. W. R. Wadt, P. J. Hay, *J. Chem. Phys.* **82** (1985) 284
12. P. J. Hay, W. R. Wadt, *J. Chem. Phys.* **82** (1985) 299
13. Š. Miertus, E. Scrocco, J. Tomasi, *Chem. Phys.* **55** (1981) 117
14. O. V. Gritsenko, P. R. T. Schipper, E. J. Baerends, *Chem. Phys. Lett.* **302** (1999) 199
15. O. V. Gritsenko, P. R. T. Schipper, E. J. Baerends, *Int. J. Quantum Chem.* **76** (2000) 407
16. *Amsterdam density functional program, Theoretical Chemistry*, Vrije Universiteit, Amsterdam, http://www.scm.com
17. G. Velde, F. M. Bickelhaupt, E. J. Baerends, C. F. Guerra, S. J. A. Gisbergen, J. G. Snijders, T. Ziegler, *J. Comput. Chem.* **22** (2001) 931
18. X. H. Yu, N. Wang, H. Q. He, L. Wang, *Spectrochim. Acta, A* **122** (2014) 283
19. S. D. Yeole, S. R. Gadre, *J. Chem. Phys.* **132** (2010) 094102-1
20. P. Manna, S. K. Seth, A. Das, J. Hemming, R. Prendergast, M. Helliwell, S. R. Choudhury, A. Frontera, S. Mukhopadhyay, *Inorg. Chem.* **51** (2012) 3557
21. P. Kar, R. Biswas, M. G. B. Drew, A. Frontera, A. Ghosh, *Inorg. Chem.* **51** (2012) 1837
22. X. H. Yu, Y. X. Zhang, J. L. Zhang, H. Q. He, L. Wang, *J. Electron Spectrosc. Relat. Phenom.* **192** (2014) 7.